Proceedings of the ASME 2012 International Design Engineering Technical Conferences & Computers and Information in Engineering Conference
IDETC/CIE 2012
August 12-15, 2012, Chicago, Illinois, USA

DETC2012-70398

FITTING WEIGHTED TOTAL LEAST-SQUARES PLANES AND PARALLEL PLANES TO SUPPORT TOLERANCING STANDARDS

Craig M Shakarji
Physical Measurement Laboratory
National Institute of Standards and Technology
Gaithersburg, Maryland 20899
craig.shakarji@nist.gov

Vijay Srinivasan
Engineering Laboratory
National Institute of Standards and Technology
Gaithersburg, Maryland 20899
vijay.srinivasan@nist.gov

ABSTRACT

We present elegant algorithms for fitting a plane, two parallel planes (corresponding to a slot or a slab) or many parallel planes in a total (orthogonal) least-squares sense to coordinate data that is weighted. Each of these problems is reduced to a simple 3×3 matrix eigenvalue/eigenvector problem or an equivalent singular value decomposition problem, which can be solved using reliable and readily available commercial software. These methods were numerically verified by comparing them with brute-force minimization searches. We demonstrate the need for such weighted total least-squares fitting in coordinate metrology to support new and emerging tolerancing standards, for instance, ISO 14405-1:2010. The widespread practice of unweighted fitting works well enough when point sampling is controlled and can be made uniform (e.g., using a discrete point contact Coordinate Measuring Machine). However, we demonstrate that nonuniformly sampled points (arising from many new measurement technologies) coupled with unweighted least-squares fitting can lead to erroneous results. When needed, the algorithms presented also solve the unweighted cases simply by assigning the value one to each weight. We additionally prove convergence from the discrete to continuous cases of least-squares fitting as the point sampling becomes dense.

1. INTRODUCTION

The need for weighted total (orthogonal distance) least-squares fitting of planes and parallel planes comes from at least two fronts: new tolerancing standards and new coordinate measuring instrumentation.

Table 1. EXAMPLES OF ISO TOLERANCING SYNTAX.

Syntax	Semantics*
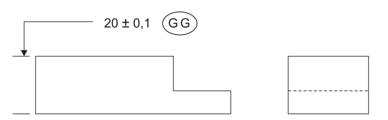	ISO 14405-1: The linear size of the indicated feature of size, with least-squares association criterion, shall be within the indicated limits.
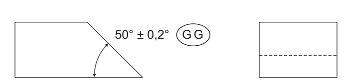	ISO 14405-3 (emerging): The angular size of the indicated feature of size, with least-squares association criterion, shall be within the indicated limits.
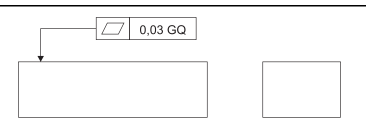	ISO 1101 (emerging): The root-mean-square parameter of any extracted (actual) surface, measured from the total least-squares associated plane, shall be less than or equal to 0,03 mm.
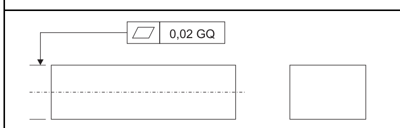	ISO 1101 (emerging): The root-mean-square parameter of extracted (actual) median plane of the indicated feature of size, measured from the total least-squares associated plane, shall be less than or equal to 0,02 mm.

* These statements of semantics are composed from different statements in ISO 14405-1:2010 and the emerging ISO 1101. These are not the formal statements of explanation associated with the drawings in the official ISO standards.

Copyright © 2012 by ASME

First, ISO tolerancing standards such as ISO 14405-1:2010 [1] and the future revisions of ISO 1101 [2], and ISO 14405-3 [3] will allow specifications to be called out based on a total least-squares criterion (see Table 1). As will be shown in Section 2, these must be interpreted as *weighted* total least-squares, where the weights are the discretely partitioned areas corresponding to the discretely sampled and measured points. Thus, there is an immediate need for weighted total least-squares fitting of planes and parallel planes.

Verification of slot and slab specifications requires fitting two parallel planes. One can also see the need for fitting several parallel planes, as in the case a door hinge [4], where there are several nominally parallel planes (perpendicular to multiple cylindrical surfaces representing holes that are nominally coaxial). Under such fitting, tolerancing a hinge can be treated as a one-dimensional tolerancing problem that is by no means trivial.

The second reason for weighted (as opposed to unweighted) total least-squares fitting arises from newer instrumentation. Discrete point Coordinate Measuring Machines (CMMs) can be programmed to sample a surface predictably and uniformly. That is, before any CMM probing occurs, the number of points and their approximate sampling pattern can already be known, and the operator generally chooses the points. This luxury allows for more or less even sampling of surfaces that are then associated with ideal form geometries based on an unweighted total least-squares fitting criterion.

But the introduction of newer measurement technologies takes away such *a priori* knowledge. An operator using—for example—an articulating arm CMM with a handheld laser scanner does not know how many points will be collected or, to a certain extent, how uniform the sampling will be (even considering deliberate attempts by the operator). The ramifications of this are important. Consider the problem of fitting two parallel planes to a slot—a task that can arise from a tolerance specification according to ISO 14405-1, which can specifically indicate a least-squares criterion. In this example, we suppose that the actual planar surfaces are not quite parallel. Figure 1 shows the effect that variations in sampling can have on the fit. In the figure, the unweighted least-squares parallel planes is shown by the dashed lines when fit to points having uniform sampling (left) and nonuniform sampling (right). (In this figure, the sampled points happen to lie exactly on the surface, but this does not affect the idea conveyed.)

As Fig. 1 shows, when the sampling is uniform, the orientation of the fit planes matches what is expected and desired, namely the orientation matches what one would get in the continuous case. But when the sampling is not uniform all over, and the number of points on one planar surface is much higher than on the other, the orientation of the fit planes is skewed, an effect that deviates from the continuous case. The use of weighted least-squares (where the weights correspond to the area around each point) avoids this effect of sampling.

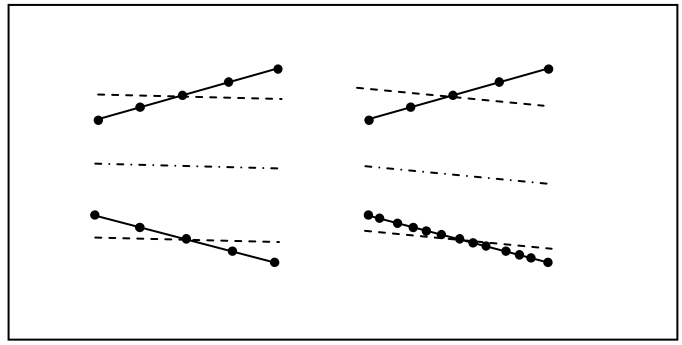

Figure 1. POINT SAMPLING DENSITY ADVERSELY AFFECTING THE LEAST-SQUARES FIT.

Note that the problem still exists when greater numbers of points are taken, provided the relative disparity remains between the numbers of points sampled on the two surfaces. And this case is realistic as optically based scanners can gather much more data on one surface than another based on various things such as distance, sampling time, lighting, and surface reflectivity.

An easily grasped example is the use of a 3D laser scanner that collects points on two nominally parallel planar surfaces of the same nominal size. If one surface is a distance of 2 m from the instrument while the other is 10 m from the instrument, the inverse square law would have us expect there to be 25 times as many points collected on the closer surface than the farther one (apart from special handling). An unweighted least-squares parallel planes fit would be almost entirely determined by the orientation of the closer plane. This could be remedied by the algorithms presented in this paper, if the points on the closer surface were given weights $1/25$ (or whatever the actual ratio of points turned out to be) of the weights given to the points on the farther surface.

The problem can exist even when fitting a single plane to points taken on one surface, if one patch is sampled more densely than the rest of the surface. The characteristics of that patch would have undue influence on the fit when using an unweighted least-squares algorithm.

While in this paper we will often associate the weights with the area of the patch of the surface corresponding to each point, the scope of this document does not include specific algorithms for calculating the weights, which is an interesting topic in itself. Further, making use of weights may be desired for other reasons such as sampled points with differing uncertainties. We also note that the case of unweighted least-squares fitting of a single plane has been well documented, for example in [5-9]. The results and proofs in this paper for single-plane fitting (Lemma 1 and Theorem 1) are straightforward extensions of work done for single plane fitting but now with weights included. An iterative search algorithm for weighted total least-squares line fitting is given in [10].

The remainder of this paper is organized as follows. Section 2 poses the problem in the continuous case and shows why this lends itself to weighted fitting in the discrete case.

 Copyright © 2012 by ASME

Section 3 gives the algorithms themselves separate from any proofs for convenient access of the reader. Section 4 contains proofs the algorithms presented. Section 5 gives Matlab[1] code of the algorithms along with results of numerical testing. Section 6 extends the algorithms to the continuous case. Section 7 contains the proof that the results from the discrete algorithms converge to their continuous counterparts as the points become dense, and Section 8 gives conclusions of this work.

2. DEFINITIONS IN CONTINUOUS CASES AND THEIR DISCRETE APPROXIMATIONS

As described in [11], to fit a total least-squares plane to a surface patch in space, we pose the following optimization problem (with reference to Fig. 2):

TlsqPlane: Given a bounded surface S, find the plane P that minimizes $\int_S d^2(\boldsymbol{p}, P)ds$.

Here $d(\boldsymbol{p}, P)$ denotes the signed perpendicular distance (hence the qualification 'total' for the least-squares fitting) of a point $\boldsymbol{p}$ on surface patch S from the plane P that will be fitted. Once such a plane P has been found, the root-mean-square parameter for the bounded surface S is given by

$$\sqrt{\frac{\int_S d^2(\boldsymbol{p}, P)ds}{\int_S ds}}. \tag{1}$$

We note that $\int_S ds$ is the area of the surface patch. If the surface consists of several patches, then the integrals can be evaluated over each patch and then summed.

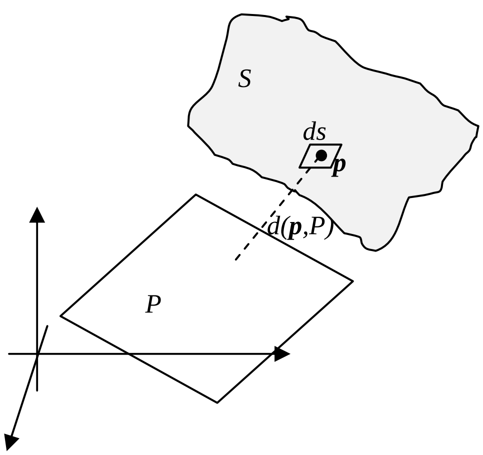

Figure 2. FITTING A PLANE TO A SURFACE PATCH.

The objective function in TlsqPlane cannot, in general, be evaluated in closed form. So we resort to numerical integration over the surface S. We can sample points on a surface patch after dividing up the patch into discrete areas ΔA_i and approximate the objective function as

$$\int_S d^2(\boldsymbol{p}, P)ds \;\approx\; \sum_{i=1}^{N} \{d^2(\boldsymbol{p}_i, P)\} \cdot \Delta A_i\,, \tag{2}$$

where $\boldsymbol{p}_i$ are the N sampled points, one in each subdivision. Thus we are led to minimizing $\sum_{i=1}^{N} [\{d^2(\boldsymbol{p}_i, P)\} \cdot \Delta A_i]$ over the parameters of the plane P for TlsqPlane, where ΔA_i's are treated as the weights.

When we need to fit two or more parallel planes, the problem can be formulated as follows. For simplicity, we will present the case of fitting two parallel planes (with corresponding illustration in Fig. 3):

TlsqParallelPlanes: Given two bounded surfaces S_1 and S_2, find two parallel planes P_1 and P_2 that minimize $\int_{S_1} d^2(\boldsymbol{p}, P_1)ds + \int_{S_2} d^2(\boldsymbol{p}, P_2)ds$.

Once such parallel planes P_1 and P_2 have been found, the distance between them is the linear size (that has been defined with the least-squares criterion) in ISO 14405-1:2010. The definition can be extended to any arbitrary number of parallel planes. A discrete approximation to the TlsqParallelPlanes problem can be defined as we did for the TlsqPlane problem.

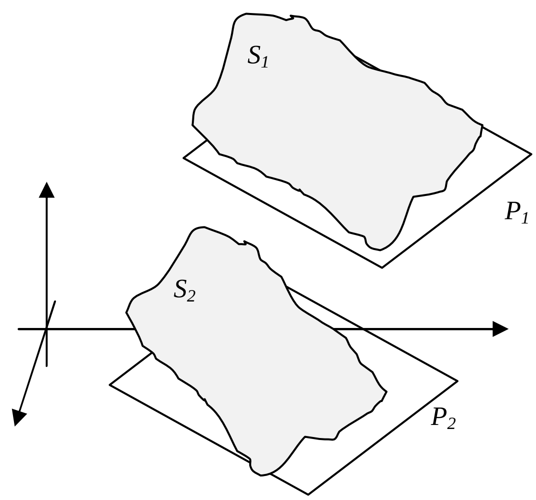

Figure 3. FITTING TWO PARALLEL PLANES.

3. FITTING ALGORITHMS

For the convenience of the reader, the algorithms themselves are presented in this section, unencumbered by their proofs, which appear later.

If a plane is defined by a point on the plane $\boldsymbol{x} = (x, y, z)$ and the direction cosines of the normal to the plane (i.e., the unit vector normal to the plane) $\boldsymbol{a} = (a, b, c)$, then the signed

[1] Certain commercial software packages are identified in this paper in order to specify the experimental procedures and code adequately. Such identification is not intended to imply recommendation or endorsement by the National Institute of Standards and Technology, nor is it intended to imply that the software tools identified are necessarily the best available for the purpose.

Copyright © 2012 by ASME

orthogonal distance from a point $\boldsymbol{x}_i = (x_i,\ y_i,\ z_i)$ to the plane is given by:

$$d_i = \boldsymbol{a} \cdot (\boldsymbol{x}_i - \boldsymbol{x}) = a(x_i - x) + b(y_i - y) + c(z_i - z).$$

3.1 Fitting a Single Plane

Given:

1) Data points $\boldsymbol{x}_1,\ \boldsymbol{x}_2,\ \boldsymbol{x}_3, \cdots,\ \boldsymbol{x}_N$, where each $\boldsymbol{x}_i = (x_i,\ y_i,\ z_i)$, and
2) The corresponding weights, $w_1,\ w_2,\ w_3, \cdots,\ w_N$, where all the weights are positive.

Then the weighted total least-squares plane is defined as the plane that minimizes $\sum_{i=1}^{N} w_i d_i^2$, where d_i is the orthogonal distance from the i^{th} data point to the plane.

The weighted total least-squares plane can be found as follows:

1) A point on the plane is the weighted centroid, namely $\bar{\boldsymbol{x}} = (\bar{x}, \bar{y}, \bar{z}) = \frac{\sum_{i=1}^{N} w_i \boldsymbol{x}_i}{\sum_{i=1}^{N} w_i}$.
2) The unit vector normal to the plane is the (right) singular vector corresponding to the smallest singular value in the singular-value decomposition (SVD) of the $N \times 3$ matrix given by:

$$\begin{bmatrix} \sqrt{w_1}(x_1 - \bar{x}) & \sqrt{w_1}(y_1 - \bar{y}) & \sqrt{w_1}(z_1 - \bar{z}) \\ \sqrt{w_2}(x_2 - \bar{x}) & \sqrt{w_2}(y_2 - \bar{y}) & \sqrt{w_2}(z_2 - \bar{z}) \\ \vdots & \vdots & \vdots \\ \sqrt{w_N}(x_N - \bar{x}) & \sqrt{w_N}(y_N - \bar{y}) & \sqrt{w_N}(z_N - \bar{z}) \end{bmatrix}.$$

The unweighted case (i.e., the equally weighted case) can be found by making the value of all the weights equal to one, thus removing their appearance from the matrix. Scaling all the weights by the any fixed, positive value does not affect the solution.

There is a close connection between the smallest singular value and the root-mean-square (RMS) value between the fitted plane and the surface (as approximated by the sampled points). This RMS value is a quantity of interest in future ISO 1101 revisions. As we will later see in the proof of Theorem 1, the square of the smallest singular value equals the objective function—the weighted sum-of-squares of residuals. If we denote the smallest singular value as σ, and if the weights correspond to the discretely partitioned areas about the sampled points, totaling A, then the (discrete) RMS value can be simply obtained as:

$$\sqrt{\frac{\sigma^2}{\sum_{i=1}^{N} w_i}} = \frac{\sigma}{\sqrt{A}}.$$

3.2 Two Parallel Planes

Given:

1) Two sets of data points $\boldsymbol{x}_1,\ \boldsymbol{x}_2,\ \cdots,\ \boldsymbol{x}_N$ and $\boldsymbol{x}_{N+1},\ \boldsymbol{x}_{N+2},\ \cdots,\ \boldsymbol{x}_{N+M}$, where each $\boldsymbol{x}_i = (x_i,\ y_i,\ z_i)$, where it is known *a priori* which points belong to each plane, and
2) The corresponding weights, $w_1,\ w_2,\ w_3, \cdots,\ w_{N+M}$, where all the weights are positive.

Then the weighted total least-squares fitting of two parallel planes (e.g., corresponding to a slot or slab) is defined as the pair of parallel planes that minimizes $\sum_{i=1}^{N+M} w_i d_i^2$, where d_i is the orthogonal distance from the i^{th} data point to the first plane when $1 \le i \le N$ or to the second plane when $N + 1 \le i \le N + M$.

If two parallel planes are defined by a point on the first plane $\boldsymbol{x_A} = (x_A, y_A, z_A)$, a point on the second plane $\boldsymbol{x_B} = (x_B, y_B, z_B)$, and the unit vector normal to the parallel planes, $\boldsymbol{a} = (a, b, c)$, then the weighted total least-squares parallel planes can be found as follows:

1) A point on the first plane is the weighted centroid of the first set of data points, namely, $\bar{\boldsymbol{x}}_{\boldsymbol{A}} = (\bar{x}_A, \bar{y}_A, \bar{z}_A) = \frac{\sum_{i=1}^{N} w_i \boldsymbol{x}_i}{\sum_{i=1}^{N} w_i}$.
2) A point on the second plane is the weighted centroid of the second set of data points, namely, $\bar{\boldsymbol{x}}_{\boldsymbol{B}} = (\bar{x}_B, \bar{y}_B, \bar{z}_B) = \frac{\sum_{i=N+1}^{N+M} w_i \boldsymbol{x}_i}{\sum_{i=N+1}^{N+M} w_i}$.
3) The unit vector normal to the plane is the singular vector corresponding to the smallest singular value of the $(N + M) \times 3$ matrix given by:

$$\begin{bmatrix} \sqrt{w_1}(x_1 - \bar{x}_A) & \sqrt{w_1}(y_1 - \bar{y}_A) & \sqrt{w_1}(z_1 - \bar{z}_A) \\ \sqrt{w_2}(x_2 - \bar{x}_A) & \sqrt{w_2}(y_2 - \bar{y}_A) & \sqrt{w_2}(z_2 - \bar{z}_A) \\ \vdots & \vdots & \vdots \\ \sqrt{w_N}(x_N - \bar{x}_A) & \sqrt{w_N}(y_N - \bar{y}_A) & \sqrt{w_N}(z_N - \bar{z}_A) \\ \sqrt{w_{N+1}}(x_{N+1} - \bar{x}_B) & \sqrt{w_{N+1}}(y_{N+1} - \bar{y}_B) & \sqrt{w_{N+1}}(z_{N+1} - \bar{z}_B) \\ \sqrt{w_{N+2}}(x_{N+2} - \bar{x}_B) & \sqrt{w_{N+2}}(y_{N+2} - \bar{y}_B) & \sqrt{w_{N+2}}(z_{N+2} - \bar{z}_B) \\ \vdots & \vdots & \vdots \\ \sqrt{w_{N+M}}(x_{N+M} - \bar{x}_B) & \sqrt{w_{N+M}}(y_{N+M} - \bar{y}_B) & \sqrt{w_{N+M}}(z_{N+M} - \bar{z}_B) \end{bmatrix}$$

The distance between the two planes can be easily calculated as $|\boldsymbol{a} \cdot (\bar{\boldsymbol{x}}_{\boldsymbol{A}} - \bar{\boldsymbol{x}}_{\boldsymbol{B}})|$.

The unweighted case (i.e., the equally weighted case) can be found by making the value of all the weights equal to one, thus removing their appearance from the matrix. Scaling all the weights (not just the weights for one plane) by the same factor does not affect the solution.

3.3 Arbitrarily Many Parallel Planes

The solution for two planes extends to arbitrarily many planes, where every plane passes through its weighted centroid,

Copyright © 2012 by ASME

and the SVD is performed on the matrix written out in Theorem 2.

4. PROOFS OF ALGORITHMS

We prove the correctness of the algorithms given in Section 3 above. Before giving lemmas and theorems, we note that the least-squares solutions might not be unique. While we do not rely on uniqueness in the proofs here, nonuniqueness arises only in pathological cases and is not a problem when we deal with planes in practical measurements on realistic parts [12]. Hence, we proceed, simply speaking of *the* least-squares plane. We start with a lemma related to the location of the weighted total least-squares plane.

Lemma 1. *Assume that we are given data points* $\boldsymbol{x}_1, \boldsymbol{x}_2, \boldsymbol{x}_3, \cdots, \boldsymbol{x}_N$, *where* $\boldsymbol{x}_i = (x_i, y_i, z_i)$, *corresponding positive weights* $w_1, w_2, w_3, \cdots, w_N$, *and an arbitrary unit normal vector,* $\boldsymbol{a} = (a, b, c)$. *Then the weighted total least-squares plane constrained to have normal* $\boldsymbol{a}$ *must pass through the weighted centroid,* $\overline{\boldsymbol{x}} = (\bar{x}, \bar{y}, \bar{z}) = \frac{\sum_{i=1}^{N} w_i \boldsymbol{x}_i}{\sum_{i=1}^{N} w_i}$. *Furthermore, any plane with normal* $\boldsymbol{a}$ *but not passing through the weighted centroid has a weighted sum-of-squares strictly greater than the plane passing through the centroid.*

Proof: The equation of any plane having normal $\boldsymbol{a}$ can be written as $\boldsymbol{a} \cdot \boldsymbol{x} - d = 0$, where d is the signed distance from the plane to the origin. The signed orthogonal distance from any arbitrary point $\boldsymbol{x}_i$ to this plane is $\boldsymbol{a} \cdot \boldsymbol{x}_i - d$. Thus the weighted sum-of-squares objective function for any plane of orientation $\boldsymbol{a}$ is given by $F(d) = \sum_{i=1}^{N} w_i (\boldsymbol{a} \cdot \boldsymbol{x}_i - d)^2$.

Taking the first and second derivatives yields:

$$F'(d) = -2 \sum_{i=1}^{N} w_i (\boldsymbol{a} \cdot \boldsymbol{x}_i - d) \text{, and}$$

$$F''(d) = 2 \sum_{i=1}^{N} w_i > 0 \text{, as all weights are positive.}$$

The fact that the second derivative is a positive constant implies that the function is strictly convex, and has a unique minimum if and where its first derivative vanishes. This occurs when $\sum_{i=1}^{N} w_i (\boldsymbol{a} \cdot \boldsymbol{x}_i - d) = 0$. Distributing the sum and solving for d yields

$$d = \frac{\sum_{i=1}^{N} w_i (\boldsymbol{a} \cdot \boldsymbol{x}_i)}{\sum_{i=1}^{N} w_i} = \boldsymbol{a} \cdot \left(\frac{\sum_{i=1}^{N} w_i \boldsymbol{x}_i}{\sum_{i=1}^{N} w_i} \right) = \boldsymbol{a} \cdot \overline{\boldsymbol{x}}.$$

But this means that the distance from $\overline{\boldsymbol{x}}$ (the weighted centroid) to the plane is $\boldsymbol{a} \cdot \overline{\boldsymbol{x}} - d = 0$, implying that the weighted centroid must lie on the weighted total least-squares plane constrained to have normal $\boldsymbol{a}$. Furthermore, the objective function is strictly convex, meaning any other plane not passing through the weighted centroid must have a greater weighted sum-of-squares. □

This result now enables us to prove a more general lemma involving multiple planes.

Lemma 2. *Assume that we are given* $K \geq 2$ *sets of data points* $\{\boldsymbol{x}_{1,1}, \boldsymbol{x}_{2,1}, \cdots, \boldsymbol{x}_{N1,1}\}$, $\{\boldsymbol{x}_{1,2}, \boldsymbol{x}_{2,2}, \cdots, \boldsymbol{x}_{N2,2}\}$, …, $\{\boldsymbol{x}_{1,2}, \boldsymbol{x}_{2,2}, \cdots, \boldsymbol{x}_{NK,K}\}$, *where each* $\boldsymbol{x}_{ij} = (x_{ij}, y_{ij}, z_{ij})$, *and the corresponding positive weights:* $w_{1,1}, w_{2,1}, \cdots w_{N1,1}, w_{1,2}, w_{2,2}, \cdots, w_{NK,K}$, *where all the weights are positive. Then a set of* K *parallel planes of weighted total least-squares has the property that each plane passes through the weighted centroid of its corresponding data set.*

Proof: For the sake of simplicity of notation and ease for the reader, we demonstrate the proof for the case of $K = 2$. The proof can be simply extended for cases of $K > 2$. Using simpler notation then, we assume two sets of data points, $\boldsymbol{x}_1, \boldsymbol{x}_2, \cdots, \boldsymbol{x}_N$, and $\boldsymbol{x}_{N+1}, \boldsymbol{x}_{N+2}, \cdots, \boldsymbol{x}_{N+M}$, and corresponding weights, $w_1, w_2, w_3, \cdots, w_{N+M}$.

The weighted sum-of-squares objective function is given by

$$F(\boldsymbol{a}, d_A, d_B) = \sum_{i=1}^{N} w_i [\boldsymbol{a} \cdot \boldsymbol{x}_i - d_A]^2 + \sum_{i=N+1}^{N+M} w_i [\boldsymbol{a} \cdot \boldsymbol{x}_i - d_B]^2.$$

(Here, d_A and d_B are the distances from the two planes to the origin.) For a fixed orientation, $\boldsymbol{a}^*$, the objective function becomes:

$$F(d_A, d_B) = \sum_{i=1}^{N} w_i [\boldsymbol{a}^* \cdot \boldsymbol{x}_i - d_A]^2 + \sum_{i=N+1}^{N+M} w_i [\boldsymbol{a}^* \cdot \boldsymbol{x}_i - d_B]^2 .$$

But we note that d_A occurs in the first sum only and d_B occurs in the second sum only, allowing us to express the objective function as $F(d_A, d_B) = F(d_A) + F(d_B)$, where $F(d_A)$ and $F(d_B)$ are defined as in the proof of Lemma 1 and each corresponding to its own set of data. This decomposition allows us to see that $F(d_A, d_B)$ is minimized when each term in its sum is minimized. That is,

$$\min_{d_A, d_B} [F(d_A, d_B)] = \min_{d_A} [F(d_A)] + \min_{d_B} [F(d_B)]. \quad (3)$$

Thus for the fixed orientation, the parallel planes minimizing the objective function are in fact the planes that each individually minimize the weighted sum-of-squares for its own set of data.

Lemma 1 can be applied then to the two minimization problems on the right hand side of Eq. (3), yielding that each plane must pass through the weighted centroid of its individual data set. Since this result is true for any fixed direction $\boldsymbol{a}^*$, it follows that it holds for the least-squares direction in particular. □

Armed with these lemmas, we can prove two theorems supporting the fitting algorithms presented in Section 3.

Theorem 1. *Assume that we are given data points* $\boldsymbol{x}_1, \boldsymbol{x}_2, \boldsymbol{x}_3, \cdots, \boldsymbol{x}_N$, *where each* $\boldsymbol{x}_i = (x_i, y_i, z_i)$, *and corresponding positive weights* $w_1, w_2, w_3, \cdots, w_N$, *then a weighted total least-squares plane can be computed as the plane passing through its weighted centroid,* $\overline{\boldsymbol{x}}$, *and having its orientation defined by the singular vector corresponding to the smallest singular value of the* $N \times 3$ *matrix*

Copyright © 2012 by ASME

$$\boldsymbol{M} = \begin{bmatrix} \sqrt{w_1}(x_1 - \bar{x}) & \sqrt{w_1}(y_1 - \bar{y}) & \sqrt{w_1}(z_1 - \bar{z}) \\ \sqrt{w_2}(x_2 - \bar{x}) & \sqrt{w_2}(y_2 - \bar{y}) & \sqrt{w_2}(z_2 - \bar{z}) \\ \vdots & \vdots & \vdots \\ \sqrt{w_N}(x_N - \bar{x}) & \sqrt{w_N}(y_N - \bar{y}) & \sqrt{w_N}(z_N - \bar{z}) \end{bmatrix}.$$

Proof: That the weighted least-squares plane passes through the weighted centroid is seen as an immediate consequence of Lemma 1. To find the orientation, we see the objective function to be minimized can be written as $F(\boldsymbol{a}) = \sum w_i[\boldsymbol{a} \cdot (\boldsymbol{x}_i - \bar{\boldsymbol{x}})]^2$, (where the sum is understood to extend over all i) subject to the constraint that $G(\boldsymbol{a}) = |\boldsymbol{a}|^2 - 1 = 0$.

We use Lagrange multipliers to note that the minimum of F—subject to the constraint—occurs when $\nabla F = \lambda \nabla G$ for some real number λ. When these partial derivatives are calculated, we find that $\nabla G = 2\boldsymbol{a}$, and that

$$\nabla F = \begin{bmatrix} \frac{\partial F}{\partial a} \\ \frac{\partial F}{\partial b} \\ \frac{\partial F}{\partial c} \end{bmatrix} = 2 \begin{bmatrix} \sum w_i[\boldsymbol{a} \cdot (\boldsymbol{x}_i - \bar{\boldsymbol{x}})]\,(x_i - \bar{x}) \\ \sum w_i[\boldsymbol{a} \cdot (\boldsymbol{x}_i - \bar{\boldsymbol{x}})]\,(y_i - \bar{y}) \\ \sum w_i[\boldsymbol{a} \cdot (\boldsymbol{x}_i - \bar{\boldsymbol{x}})]\,(z_i - \bar{z}) \end{bmatrix},$$

which can be rewritten as

$$2 \begin{bmatrix} \sum w_i(x_i - \bar{x})^2 & \sum w_i(x_i - \bar{x})(y_i - \bar{y}) & \sum w_i(x_i - \bar{x})(z_i - \bar{z}) \\ \sum w_i(x_i - \bar{x})(y_i - \bar{y}) & \sum w_i(y_i - \bar{y})^2 & \sum w_i(y_i - \bar{y})(z_i - \bar{z}) \\ \sum w_i(x_i - \bar{x})(z_i - \bar{z}) & \sum w_i(y_i - \bar{y})(z_i - \bar{z}) & \sum w_i(z_i - \bar{z})^2 \end{bmatrix} \begin{bmatrix} a \\ b \\ c \end{bmatrix}.$$

If we denote this 3×3 matrix (without the multiplying coefficient 2) as $\boldsymbol{L}$, we find that $\nabla F = \lambda \nabla G$ can be written as the elegant eigen-problem:

$$\boldsymbol{L} \begin{bmatrix} a \\ b \\ c \end{bmatrix} = \lambda \begin{bmatrix} a \\ b \\ c \end{bmatrix}.$$

The orientation, (a, b, c), can now be found solving this 3×3 eigenvector problem by using well known methods (e.g., Jacobi iterations) or by using solvers in higher level languages.

However, we note further that the symmetric matrix above can be written as $\boldsymbol{M}^{\mathrm{T}}\boldsymbol{M}$, where $\boldsymbol{M}$ is defined above in the theorem statement. The eigenvectors of $\boldsymbol{M}^{\mathrm{T}}\boldsymbol{M}$ are also the singular vectors of $\boldsymbol{M}$. This allows us to gain better numerical results by applying the SVD to $\boldsymbol{M}$ without ever computing $\boldsymbol{M}^{\mathrm{T}}\boldsymbol{M}$.

Finally, we must determine how to select the correct eigenvector (i.e., singular vector) of the three produced by the SVD. The normal equations can be written as follows:

$$\sum w_i(x_i - \bar{x})[\boldsymbol{a} \cdot (\boldsymbol{x}_i - \bar{\boldsymbol{x}})] = \lambda a$$
$$\sum w_i(y_i - \bar{y})[\boldsymbol{a} \cdot (\boldsymbol{x}_i - \bar{\boldsymbol{x}})] = \lambda b$$
$$\sum w_i(z_i - \bar{z})[\boldsymbol{a} \cdot (\boldsymbol{x}_i - \bar{\boldsymbol{x}})] = \lambda c.$$

Multiplying these equations by $a, b,$ and c respectively, and then summing the equations gives $\sum w_i[\boldsymbol{a} \cdot (\boldsymbol{x}_i - \bar{\boldsymbol{x}})]^2 = \lambda|\boldsymbol{a}|^2 = \lambda$.

But the sum on the left is exactly the objective function, $F(\boldsymbol{a})$, hence the correct eigenvector for the solution corresponds to the smallest eigenvalue (since $F(\boldsymbol{a}) = \lambda$, and we seek to minimize F). When using the SVD, we choose the singular vector corresponding to the smallest singular value, since under these conditions the singular values are the square roots of the eigenvalues. □

While this paper deals with planes, we note that the weighted total least-squares line in space can be found in an almost identical fashion. The weighted centroid lies on the solution line, and the orientation of the line in space can be found by choosing the singular vector corresponding to the largest singular value of $\boldsymbol{M}$.

The next theorem deals with fitting parallel planes. It is a pleasing result that the fitting of parallel planes turns out to be solved by such an easy-to-implement extension of the already-elegant single plane case.

Theorem 2. *Assume that we are given K sets of data points $\{\boldsymbol{x}_{1,1}, \boldsymbol{x}_{2,1}, \cdots, \boldsymbol{x}_{N1,1}\}$, $\{\boldsymbol{x}_{1,2}, \boldsymbol{x}_{2,2}, \cdots, \boldsymbol{x}_{N2,2}\}$, …, $\{\boldsymbol{x}_{1,2}, \boldsymbol{x}_{2,2}, \cdots, \boldsymbol{x}_{NK,K}\}$, where $\boldsymbol{x}_{ij} = (x_{ij}, y_{ij}, z_{ij})$, and the corresponding positive weights: $w_{1,1}, w_{2,1}, \cdots w_{N1,1}, w_{1,2}, w_{2,2}, \cdots, w_{NK,K}$, where all the weights are positive. Then a set of K parallel planes of weighted total least-squares can be computed as the planes passing through the respective weighted centroids of the data sets and all sharing the same orientation defined by the singular vector corresponding to the smallest singular value of the matrix*

$$\begin{bmatrix} \sqrt{w_{1,1}}(x_{1,1} - \bar{x}_{A1}) & \sqrt{w_{1,1}}(y_{1,1} - \bar{y}_{A1}) & \sqrt{w_{1,1}}(z_{1,1} - \bar{z}_{A1}) \\ \sqrt{w_{2,1}}(x_{2,1} - \bar{x}_{A1}) & \sqrt{w_{2,1}}(y_{2,1} - \bar{y}_{A1}) & \sqrt{w_{2,1}}(z_{2,1} - \bar{z}_{A1}) \\ \vdots & \vdots & \vdots \\ \sqrt{w_{N1,1}}(x_{N1,1} - \bar{x}_{A1}) & \sqrt{w_{N,1}}(y_{N1,1} - \bar{y}_{A1}) & \sqrt{w_{N1,1}}(z_{N1,1} - \bar{z}_{A1}) \\ \sqrt{w_{1,2}}(x_{1,2} - \bar{x}_{A2}) & \sqrt{w_{1,2}}(y_{1,2} - \bar{y}_{A2}) & \sqrt{w_{1,2}}(z_{N+1} - \bar{z}_{A2}) \\ \sqrt{w_{2,2}}(x_{2,2} - \bar{x}_{A2}) & \sqrt{w_{2,2}}(y_{2,2} - \bar{y}_{A2}) & \sqrt{w_{2,2}}(z_{N+2} - \bar{z}_{A2}) \\ \vdots & \vdots & \vdots \\ \sqrt{w_{NK,K}}(x_{NK,K} - \bar{x}_{AK}) & \sqrt{w_{NK,K}}(y_{NK,K} - \bar{y}_{AK}) & \sqrt{w_{NK,K}}(z_{NK,K} - \bar{z}_{AK}) \end{bmatrix}.$$

Proof: For the sake of simplicity of notation and ease for the reader, we demonstrate the proof for the case of $K = 2$, as we did in Lemma 2. Using simpler notation then, we assume two sets of data points, $\boldsymbol{x}_1, \boldsymbol{x}_2, \cdots, \boldsymbol{x}_N$, and $\boldsymbol{x}_{N+1}, \boldsymbol{x}_{N+2}, \cdots, \boldsymbol{x}_{N+M}$, and corresponding weights, $w_1, w_2, w_3, \cdots, w_{N+M}$.

That each plane passes through the weighted centroid of its respective data set is an immediate consequence of Lemma 2. We denote these weighted centroids as $\bar{\boldsymbol{x}}_{\boldsymbol{A}}$ and $\bar{\boldsymbol{x}}_{\boldsymbol{B}}$, respectively. Knowing this, the objective function to be minimized can be written as a function of $\boldsymbol{a}$ alone:

$$F(\boldsymbol{a}) = \sum_{i=1}^{N} w_i[\boldsymbol{a} \cdot (\boldsymbol{x}_i - \bar{\boldsymbol{x}}_{\boldsymbol{A}})]^2 + \sum_{i=N+1}^{N+M} w_i[\boldsymbol{a} \cdot (\boldsymbol{x}_i - \bar{\boldsymbol{x}}_{\boldsymbol{B}})]^2.$$

Copyright © 2012 by ASME

To solve the orientation problem, we again use the method of Lagrange multipliers. The minimum of $F(\boldsymbol{a})$ subject to $G(\boldsymbol{a})=0$ (where $G(\boldsymbol{a})=|\boldsymbol{a}|^2-1$) occurs when $\nabla F=\lambda\nabla G$. In this case we have,

$$\nabla F=\begin{bmatrix}\frac{\partial F}{\partial a}\\ \frac{\partial F}{\partial b}\\ \frac{\partial F}{\partial c}\end{bmatrix},$$

which, when expanded becomes:

$$2\begin{bmatrix}\sum_{i=1}^{N} w_i[\boldsymbol{a}\cdot(\boldsymbol{x}_i-\bar{\boldsymbol{x}}_A)](x_i-\bar{x}_A)+\sum_{i=N+1}^{N+M} w_i[\boldsymbol{a}\cdot(\boldsymbol{x}_i-\bar{\boldsymbol{x}}_B)](x_i-\bar{x}_B)\\ \sum_{i=1}^{N} w_i[\boldsymbol{a}\cdot(\boldsymbol{x}_i-\bar{\boldsymbol{x}}_A)](y_i-\bar{y}_A)+\sum_{i=N+1}^{N+M} w_i[\boldsymbol{a}\cdot(\boldsymbol{x}_i-\bar{\boldsymbol{x}}_B)](y_i-\bar{y}_B)\\ \sum_{i=1}^{N} w_i[\boldsymbol{a}\cdot(\boldsymbol{x}_i-\bar{\boldsymbol{x}}_A)](z_i-\bar{z}_A)+\sum_{i=N+1}^{N+M} w_i[\boldsymbol{a}\cdot(\boldsymbol{x}_i-\bar{\boldsymbol{x}}_B)](z_i-\bar{z}_B)\end{bmatrix}$$

Similar to the single plane case, computing the gradients yields an eigenvector problem, but the sum in each matrix entry is replaced by the two corresponding sums for data sets A and B.

As in the proof of Theorem 1, we have $\nabla G=2\boldsymbol{a}$ and $\nabla F=2\boldsymbol{L}\boldsymbol{a}=2(\boldsymbol{M}^T\boldsymbol{M})\boldsymbol{a}$, where $\boldsymbol{L}$ is defined to be $\boldsymbol{M}^T\boldsymbol{M}$, and where $\boldsymbol{M}$ is now defined as the $(N+M)\times 3$ matrix given as

$$\begin{bmatrix}\sqrt{w_1}(x_1-\bar{x}_A) & \sqrt{w_1}(y_1-\bar{y}_A) & \sqrt{w_1}(z_1-\bar{z}_A)\\ \sqrt{w_2}(x_2-\bar{x}_A) & \sqrt{w_2}(y_2-\bar{y}_A) & \sqrt{w_2}(z_2-\bar{z}_A)\\ \vdots & \vdots & \vdots\\ \sqrt{w_N}(x_N-\bar{x}_A) & \sqrt{w_N}(y_N-\bar{y}_A) & \sqrt{w_N}(z_N-\bar{z}_A)\\ \sqrt{w_{N+1}}(x_{N+1}-\bar{x}_B) & \sqrt{w_{N+1}}(y_{N+1}-\bar{y}_B) & \sqrt{w_{N+1}}(z_{N+1}-\bar{z}_B)\\ \sqrt{w_{N+2}}(x_{N+2}-\bar{x}_B) & \sqrt{w_{N+2}}(y_{N+2}-\bar{y}_B) & \sqrt{w_{N+2}}(z_{N+2}-\bar{z}_B)\\ \vdots & \vdots & \vdots\\ \sqrt{w_{N+M}}(x_{N+M}-\bar{x}_B) & \sqrt{w_{N+M}}(y_{N+M}-\bar{y}_B) & \sqrt{w_{N+M}}(z_{N+M}-\bar{z}_B)\end{bmatrix}.$$

The orientation, (a,b,c), can be found by solving the 3×3 eigen-problem given by $\boldsymbol{L}\begin{bmatrix}a\\b\\c\end{bmatrix}=\lambda\begin{bmatrix}a\\b\\c\end{bmatrix}$, by using well known methods .

As in the proof of Theorem 1, the eigenvectors of $\boldsymbol{M}^T\boldsymbol{M}$ are also the singular vectors of $\boldsymbol{M}$. This allows us to gain better numerical results by applying the SVD to $\boldsymbol{M}$ without ever computing $\boldsymbol{M}^T\boldsymbol{M}$.

We further mimic the proof of Theorem 1 to select the proper eigenvector (singular vector). The normal equations can be written as follows:

$$\begin{aligned}\sum_{i=1}^{N} w_i(x_i-\bar{x})[\boldsymbol{a}\cdot(\boldsymbol{x}_i-\bar{\boldsymbol{x}}_A)]+\sum_{i=N+1}^{N+M} w_i(x_i-\bar{x})[\boldsymbol{a}\cdot(\boldsymbol{x}_i-\bar{\boldsymbol{x}}_B)]=\lambda a\\ \sum_{i=1}^{N} w_i(y_i-\bar{y})[\boldsymbol{a}\cdot(\boldsymbol{x}_i-\bar{\boldsymbol{x}}_A)]+\sum_{i=N+1}^{N+M} w_i(y_i-\bar{y})[\boldsymbol{a}\cdot(\boldsymbol{x}_i-\bar{\boldsymbol{x}}_B)]=\lambda b\\ \sum_{i=1}^{N} w_i(z_i-\bar{z})[\boldsymbol{a}\cdot(\boldsymbol{x}_i-\bar{\boldsymbol{x}}_A)]+\sum_{i=N+1}^{N+M} w_i(z_i-\bar{z})[\boldsymbol{a}\cdot(\boldsymbol{x}_i-\bar{\boldsymbol{x}}_B)]=\lambda c\end{aligned}$$

Multiplying these equations by $a, b,$ and c respectively, then summing the equations gives

$$\sum_{i=1}^{N} w_i[\boldsymbol{a}\cdot(\boldsymbol{x}_i-\bar{\boldsymbol{x}}_{\boldsymbol{A}})]^2+\sum_{i=N+1}^{N+M} w_i[\boldsymbol{a}\cdot(\boldsymbol{x}_i-\bar{\boldsymbol{x}}_{\boldsymbol{B}})]^2=\lambda|\boldsymbol{a}|^{\mathbf{2}}=\lambda$$

But the sum on the left is just the objective function, $F(\boldsymbol{a})$, hence the correct eigenvector for the solution corresponds to the smallest eigenvalue (since $F(\boldsymbol{a})=\lambda$, and since we seek to minimize F). When using the SVD, we choose the singular vector corresponding to the smallest singular value, since under these conditions the singular values are the square roots of the eigenvalues. □

5. MATLAB CODE AND NUMERICAL TESTING

Matlab code for the cases of fitting one or two planes is included here. The function names should be understood as `wtlsqPlane` = "weighted total least-squares plane," and `wtlsq2pp` = "weighted total least-squares two parallel planes." In this code, `w1` and `w2` are column vectors of weights. `pts1` and `pts2` are matrices three columns wide containing the coordinates of the points, one point per row. `q` is a point on the single least-squares plane; `q1` and `q2` are points on the two parallel least-squares planes. In both cases, `v` is the unit vector normal to the least-squares plane(s). The distance between the least-squares parallel planes can be computed as `abs((q1-q2)*v)`.

```
function [q, v] = wtlsqPlane(w1, pts1)

  q = sum(bsxfun(@times,w1,pts1))/sum(w1);
  A1 = bsxfun(@minus,pts1,q);

  A = [bsxfun(@times,sqrt(w1),A1)];

  [U,S,V] = svd(A,0); % Can use [V, S] = eig(A'*A);
  [s, i] = min(diag(S));
  v = V(:, i);
return;


function [q1, q2, v] = wtlsq2pp(w1, pts1, w2, pts2)

  q1 = sum(bsxfun(@times,w1,pts1))/sum(w1);
  q2 = sum(bsxfun(@times,w2,pts2))/sum(w2);

  A1 = bsxfun(@minus,pts1,q1);
  A2 = bsxfun(@minus,pts2,q2);

  A = [bsxfun(@times,sqrt(w1),A1); ...
       bsxfun(@times,sqrt(w2),A2)];

  [U, S, V] = svd(A,0); % Can use [V, S] = eig(A'*A);
  [s, i] = min(diag(S));
  v = V(:, i);
return;
```

The algorithms in this paper were also implemented in Mathematica for the cases of fitting one, two, and three parallel planes. The Matlab and Mathematica algorithms were compared with each other to assure they give the same results (up to computational precision limits). The Mathematica code

Copyright © 2012 by ASME

was also used to test the algorithms presented in this paper against a brute-force minimization search algorithm.

Test data sets were simulated randomly. Planar data sets were generated having varying aspect ratios, varying distances between them, varying numbers of points per plane, varying weights assigned, varying perturbations of the points from an exact plane, and varying nominal orientations of the planes to one another.

The brute force iterative search was performed using Mathematica's `FindMinimum` function. The options were tweaked to improve the desired accuracy and increase the working precision beyond machine precision in seeking accurate answers. The required initial guess for the function was obtained using knowledge of how the test data sets were generated. In contrast to the iterative search method, the algorithms presented in this paper were coded using normal machine precision, purposely not taking advantage of Mathematica's ability to increase the precision.

Results are shown here for the cases of two parallel planes for 100 simulated data sets. Figure 4 shows a histogram of the anglular differences between the normal directions computed by the two methods. Figure 5 shows a histogram of the relative distances between the two computed parallel plane pairs. In both figures, the deviations are given on a log base 10 scale, meaning the greatest deviation shown in Fig. 4 is 10^{-15} radians and the greatest deviation shown in Fig. 5 is 10^{-14} mm. The magnitudes of these maximum deviations are more important than the histograms themselves, since they show that in all of the cases tested, the two methods agreed to within amounts attributable to machine precision.

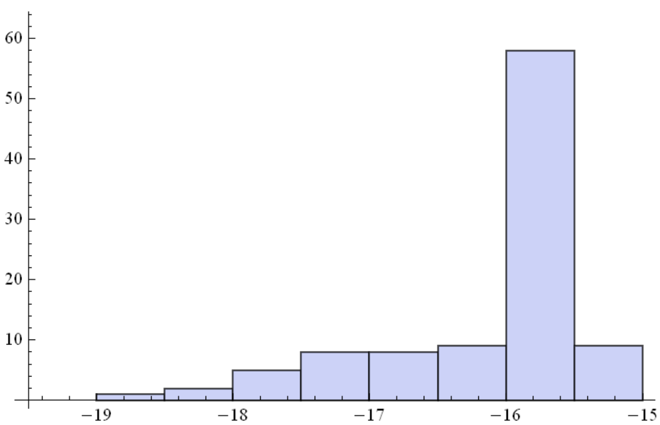

Figure 4. HISTOGRAM OF ANGULAR DEVIATIONS IN RADIANS (LOG BASE 10 SCALING).

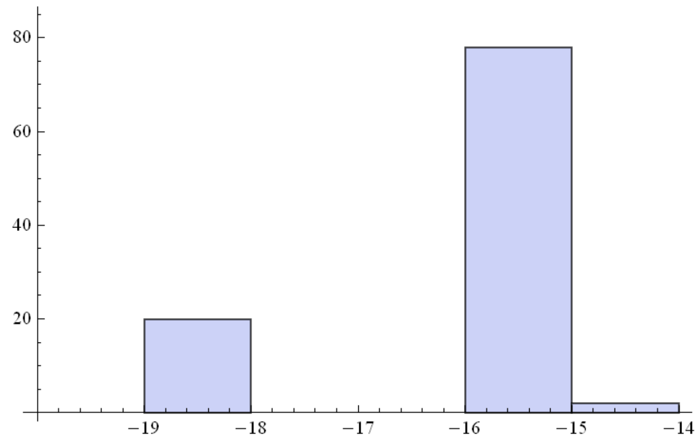

Figure 5. HISTOGRAM OF RELATIVE DISTANCE DEVIATIONS (mm, LOG BASE 10 SCALING).

6. EXTENSIONS TO CONTINUOUS CASES

The preceding work has important extensions to the continuous cases. We begin with a lemma before giving the general theorem for the continuous extension.

Lemma 3. *Assume that we are given a bounded, piecewise continuous surface, S of finite area, and an orientation,* $\boldsymbol{a}$. *Then the total least-squares plane constrained to have normal* $\boldsymbol{a}$ *must pass through the centroid,* $\bar{\boldsymbol{x}} = (\bar{x}, \bar{y}, \bar{z})$, *where* $\bar{x} = \frac{\int_S x\, ds}{\int_S ds}$, $\bar{y} = \frac{\int_S y\, ds}{\int_S ds}$, *and* $\bar{z} = \frac{\int_S z\, ds}{\int_S ds}$. *Furthermore, any plane with normal* $\boldsymbol{a}$ *but not passing through the centroid has a weighted sum-of-squares strictly greater than the plane passing through the centroid.*

Proof: The equation of any plane having normal $\boldsymbol{a}$ can be written as $\boldsymbol{a} \cdot \boldsymbol{x} - d = 0$, where d is the signed distance from the plane to the origin. The orthogonal distance from any arbitrary point $\boldsymbol{p}$ to this plane is $\boldsymbol{a} \cdot \boldsymbol{p} - d$. Thus the objective function for any plane of orientation $\boldsymbol{a}$ is given by $F(d) = \int_S [\boldsymbol{a} \cdot \boldsymbol{p} - d]^2 ds$.

Taking the first and second derivatives yields:

$$F'(d) = -2 \int_S [\boldsymbol{a} \cdot \boldsymbol{p} - d] ds \text{, and}$$
$$F''(d) = 2 \int_S ds > 0.$$

The fact that the second derivative is a positive constant implies that the function is strictly convex and has a unique minimum if and where its first derivative vanishes. This occurs when $\int_S [\boldsymbol{a} \cdot \boldsymbol{p} - d] ds = 0$. Distributing the integral and solving for d yields

$$d = \frac{\int_S [\boldsymbol{a} \cdot \boldsymbol{p}] ds}{\int_S ds} = \boldsymbol{a} \cdot \left(\frac{\int_S \boldsymbol{p} ds}{\int_S ds} \right) = \boldsymbol{a} \cdot \bar{\boldsymbol{x}}.$$

Copyright © 2012 by ASME

But this means that that the distance from $\bar{\boldsymbol{x}}$ (the centroid) to the plane, which is $\boldsymbol{a} \cdot \bar{\boldsymbol{x}} - d$, is equal to zero, implying that the centroid must lie on the total least-squares plane constrained to have normal $\boldsymbol{a}$. Furthermore, the objective function is strictly convex, meaning any other plane not passing through the centroid must have a greater objective function value. □

Theorem 3. *Assume that we are given K surfaces, $S_1, S_2, \dots, S_K$, where each surface is bounded, piecewise continuous, of finite area, and each S_i having centroid $\bar{\boldsymbol{x}}_i = (\bar{x}_i, \bar{y}_i, \bar{z}_i)$. Then a set of K parallel planes of total least-squares can be computed as the planes passing through the respective centroids of the surfaces and all sharing the same orientation defined by the eigenvector corresponding to the smallest eigenvalue of the 3×3 matrix (written as a sum of matrices for reasons of space):*

$$\sum_{i=1}^{K} \begin{bmatrix} \int_{S_i} (x-\bar{x}_i)^2 ds & \int_{S_i} (x-\bar{x}_i)(y-\bar{y}_i) ds & \int_{S_i} (x-\bar{x}_i)(z-\bar{z}_i) ds \\ \int_{S_i} (x-\bar{x}_i)(y-\bar{y}_i) ds & \int_{S_i} (y-\bar{y}_i)^2 ds & \int_{S_i} (y-\bar{y}_i)(z-\bar{z}_i) ds \\ \int_{S_i} (x-\bar{x}_i)(z-\bar{z}_i) ds & \int_{S_i} (y-\bar{y}_i)(z-\bar{z}_i) ds & \int_{S_i} (z-\bar{z}_i)^2 ds \end{bmatrix}$$

Proof: For the sake of simplicity of notation and ease for the reader, we demonstrate the proof for the case of $K = 2$, as we did in Theorem 2. Using simpler notation then, we assume two surfaces, S_A and S_B.

If two parallel planes have normal orientation $\boldsymbol{a}$ and pass through the points $\boldsymbol{x_A}$ and $\boldsymbol{x_B}$, then the objective function to be minimized is

$$F(\boldsymbol{a}, \boldsymbol{x_A}, \boldsymbol{x_B}) = \int_{S_A} [\boldsymbol{a} \cdot (\boldsymbol{p} - \boldsymbol{x_A})]^2 ds + \int_{S_B} [\boldsymbol{a} \cdot (\boldsymbol{p} - \boldsymbol{x_B})]^2 ds.$$

Since $\boldsymbol{x_A}$ occurs in the first integral only, and $\boldsymbol{x_B}$ occurs in the second integral only, then for any fixed orientation $\boldsymbol{a}$ we see that the minimization problem can be separated into two minimization problems as:

$$\min_{x_A, x_B} [F(x_A, x_B)] = \min_{x_A} [F(x_A)] + \min_{x_B} [F(x_B)]. \qquad (4)$$

This means that Lemma 3 can be applied to each minimization on the right hand side of Eq (4) indicating to us that when fitting parallel planes, each least-squares plane passes through the centroid of its respective surface. We denote these centroids as $\bar{\boldsymbol{x}}_{\boldsymbol{A}}$, and $\bar{\boldsymbol{x}}_{\boldsymbol{B}}$, respectively. Knowing this, the objective function to be minimized can be written as a function of $\boldsymbol{a}$ alone:

$$F(\boldsymbol{a}) = \int_{S_A} [\boldsymbol{a} \cdot (\boldsymbol{p} - \bar{\boldsymbol{x}}_{\boldsymbol{A}})]^2 ds + \int_{S_B} [\boldsymbol{a} \cdot (\boldsymbol{p} - \bar{\boldsymbol{x}}_{\boldsymbol{B}})]^2 ds.$$

To solve the orientation problem, we again use the method of Lagrange multipliers. The minimum of $F(\boldsymbol{a})$ subject to $G(\boldsymbol{a}) = 0$ (where $G(\boldsymbol{a}) = |\boldsymbol{a}|^2 - 1$) occurs when $\nabla F = \lambda \nabla G$. In this case,

$$\nabla F = \begin{bmatrix} \frac{\partial F}{\partial a} \\ \frac{\partial F}{\partial b} \\ \frac{\partial F}{\partial c} \end{bmatrix}$$

$$= 2 \begin{bmatrix} \int_{S_A} [\boldsymbol{a} \cdot (\boldsymbol{p} - \bar{\boldsymbol{x}}_{\boldsymbol{A}})](x - \bar{x}_A) ds + \int_{S_B} [\boldsymbol{a} \cdot (\boldsymbol{p} - \bar{\boldsymbol{x}}_{\boldsymbol{B}})](x - \bar{x}_B) ds \\ \int_{S_A} [\boldsymbol{a} \cdot (\boldsymbol{p} - \bar{\boldsymbol{x}}_{\boldsymbol{A}})](y - \bar{y}_A) ds + \int_{S_B} [\boldsymbol{a} \cdot (\boldsymbol{p} - \bar{\boldsymbol{x}}_{\boldsymbol{B}})](y - \bar{y}_B) ds \\ \int_{S_A} [\boldsymbol{a} \cdot (\boldsymbol{p} - \bar{\boldsymbol{x}}_{\boldsymbol{A}})](z - \bar{z}_A) ds + \int_{S_B} [\boldsymbol{a} \cdot (\boldsymbol{p} - \bar{\boldsymbol{x}}_{\boldsymbol{B}})](z - \bar{z}_B) ds \end{bmatrix}$$

Let $\boldsymbol{L}$ denote the 3×3 matrix (written as a sum of two matrices for reasons of space):

$$\begin{bmatrix} \int_{S_A} (x-\bar{x}_A)^2 ds & \int_{S_A} (x-\bar{x}_A)(y-\bar{y}_A) ds & \int_{S_A} (x-\bar{x}_A)(z-\bar{z}_A) ds \\ \int_{S_A} (x-\bar{x}_A)(y-\bar{y}_A) ds & \int_{S_A} (y-\bar{y}_A)^2 ds & \int_{S_A} (y-\bar{y}_A)(z-\bar{z}_A) ds \\ \int_{S_A} (x-\bar{x}_A)(z-\bar{z}_A) ds & \int_{S_A} (y-\bar{y}_A)(z-\bar{z}_A) ds & \int_{S_A} (z-\bar{z}_A)^2 ds \end{bmatrix}$$
$$+$$
$$\begin{bmatrix} \int_{S_B} (x-\bar{x}_B)^2 ds & \int_{S_B} (x-\bar{x}_B)(y-\bar{y}_B) ds & \int_{S_B} (x-\bar{x}_B)(z-\bar{z}_B) ds \\ \int_{S_B} (x-\bar{x}_B)(y-\bar{y}_B) ds & \int_{S_B} (y-\bar{y}_B)^2 ds & \int_{S_B} (y-\bar{y}_B)(z-\bar{z}_B) ds \\ \int_{S_B} (x-\bar{x}_B)(z-\bar{z}_B) ds & \int_{S_B} (y-\bar{y}_B)(z-\bar{z}_B) ds & \int_{S_B} (z-\bar{z}_B)^2 ds \end{bmatrix},$$

Then the orientation of the least-squares planes arising from $\nabla F = \lambda \nabla G$ can be written as the elegant eigen-problem:

$$\boldsymbol{L} \begin{bmatrix} a \\ b \\ c \end{bmatrix} = \lambda \begin{bmatrix} a \\ b \\ c \end{bmatrix}.$$

We mimic the proof of Theorem 1 to select the proper eigenvector. The normal equations can be written as follows:

$$\int_{S_A} [\boldsymbol{a} \cdot (\boldsymbol{p} - \bar{\boldsymbol{x}}_{\boldsymbol{A}})](x - \bar{x}_A) ds + \int_{S_B} [\boldsymbol{a} \cdot (\boldsymbol{p} - \bar{\boldsymbol{x}}_{\boldsymbol{B}})](x - \bar{x}_B) ds = \lambda a$$
$$\int_{S_A} [\boldsymbol{a} \cdot (\boldsymbol{p} - \bar{\boldsymbol{x}}_{\boldsymbol{A}})](y - \bar{y}_A) ds + \int_{S_B} [\boldsymbol{a} \cdot (\boldsymbol{p} - \bar{\boldsymbol{x}}_{\boldsymbol{B}})](y - \bar{y}_B) ds = \lambda b$$
$$\int_{S_A} [\boldsymbol{a} \cdot (\boldsymbol{p} - \bar{\boldsymbol{x}}_{\boldsymbol{A}})](z - \bar{z}_A) ds + \int_{S_B} [\boldsymbol{a} \cdot (\boldsymbol{p} - \bar{\boldsymbol{x}}_{\boldsymbol{B}})](z - \bar{z}_B) ds = \lambda c$$

Multiplying these equations by $a, b,$ and c respectively, then summing the equations gives

$$\int_{S_A} [\boldsymbol{a} \cdot (\boldsymbol{p} - \bar{\boldsymbol{x}}_{\boldsymbol{A}})]^2 ds + \int_{S_B} [\boldsymbol{a} \cdot (\boldsymbol{p} - \bar{\boldsymbol{x}}_{\boldsymbol{B}})]^2 ds = \lambda |\boldsymbol{a}|^2 = \lambda$$

But the sum on the left is just the objective function, $F(\boldsymbol{a})$, hence the correct eigenvector for the solution corresponds to the smallest eigenvalue (since $F(\boldsymbol{a}) = \lambda$, and since we seek to minimize F). □

Copyright © 2012 by ASME

7. CONVERGENCE OF THE DISCRETE TO CONTINUOUS CASE

Tolerance specifications according to standards are considered to apply to the continuous surface. Verification of such specifications is done using discrete points. Thus the fundamental connection between the discrete and continuous cases must be assured. Specifically, the discrete case should converge to the continuous case as the sampled points become dense (under idealized conditions of no measurement error).

We seek to prove convergence for surfaces over which 2nd degree polynomials (as encountered in the continuous case in Theorem 3) are Riemann integrable—surfaces that are piecewise smooth, bounded, having finite area—conditions that are reasonable for real workpieces.[2] In order to prove that the discrete solution converges to the continuous solution as the points become dense (when the weights are assigned the values of the areas of the surface corresponding to the points, as shown in Section 2) we show the following two steps:

1) Every individual cell value of the 3×3 matrix in the discrete case (denoted $\boldsymbol{L}$ in the proof of Theorem 2) converges to its corresponding cell value in the matrix in the continuous case (also denoted $\boldsymbol{L}$ in the proof of Theorem 3) as the points become dense.
2) The fact that the individual cell values converge implies that the eigenvalues and eigenvectors from the discrete case also converge to their continuous case counterparts as the points become dense.

Step 1: That the sum converges to the surface integral for each of the nine cells is immediate from the definition of the Riemann surface integral (see, e.g., 1.5.1 in [13]). Specifically then, if a partition of a surface called S is given by $S^{(n)} = \left\{S_1^{(n)}, S_2^{(n)}, \dots, S_n^{(n)}\right\}$ where these disjoint subsets have well defined areas, and if n points are chosen such that $\boldsymbol{x_i} \in S_i^{(n)}$, for $i = 1, 2, \dots, n$, then the Riemann sum for a real valued function f over S is defined by

$$R_n = \sum_{i=1}^{n} \left(\Delta A_i^{(n)}\right) f(\boldsymbol{x_i}), \tag{5}$$

where $\Delta A_i^{(n)}$ represents the area of the subset $S_i^{(n)}$. If all sequences $\{R_n\}$ approach the same limit R with $\Delta_n := \max\left\{\text{Area}\left(S_1^{(n)}\right), \dots, \text{Area}\left(S_n^{(n)}\right)\right\} \to 0$ as $n \to \infty$, then f is defined as *Riemann integrable* over S and the surface integral of f over S is defined by $\int_S f(\boldsymbol{x}) dS := R$.

In our discrete case, each cell in the matrix $\boldsymbol{L}$ contains one or more sums of the form $\sum_{i=1}^{N} w_i f(\boldsymbol{x_i})$. But since we are assigning each w_i to have the value of its point's associated area, we have in fact a Riemann sum as in Eq. (5). Futhermore, as the points become dense, we then have a sequence of Riemann sums where the maximum area of a partition approaches zero. Then by definition, this must converge to its corresponding integral when the function is integrable over S. However, since the function f is simply a second degree polynomial, it is uniformily continuous over the piecewise smooth S and thus is integrable. Hence Step 1 is shown.

Step 2: We now show that, since the individual cell values converge, the smallest eigenvalue and its corresponding eigenvector converge as well (when the smallest eigenvalue is unique, i.e., simple).

We first note that since there are a finite number of cells (namely nine) the convergence is uniform. That is, for any $\epsilon > 0$ the points will become dense enough that every cell in the discrete case differs from the continuous case by less than ϵ. We look at the sensitivities of the eigenvalues and eigenvectors in this case. Since the matrix is symmetric, we gain the advantage of several theorems that bound the changes in eigenvalues and eigenvectors under small changes to the matrix.

First, in this symmetric case, Stewart shows (p. 309 of [14]) that the eigenvalues are perfectly conditioned—that sufficiently small ϵ-sized perturbations in the cells of the matrix yield differences in the eigenvalues essentially no greater than ϵ. Thus convergence of eigenvalues is assured. Furthermore, this ensures that if the smallest eigenvalue in the continuous case is unique, then the smallest eigenvalue in the discrete case will eventually be as well.

It is also shown (p. 310 of [14]; see also [15, 16]) that the eigenvector associated with the smallest (unique) eigenvalue, λ, is also well conditioned. Specifically, if the unit eigenvector associated with the smallest eigenvalue of the matrix $\boldsymbol{L}$ is denoted $\boldsymbol{v}$, and the corresponding unit eigenvector of matrix $\boldsymbol{L} + \Delta\boldsymbol{L}$ is $\boldsymbol{v} + \Delta\boldsymbol{v}$, then the size of $\Delta\boldsymbol{v}$ is bounded as follows:

$$\|\Delta\boldsymbol{v}\|_2 \leq \frac{\|\Delta\boldsymbol{L}\|_2}{\min\left|\lambda - \lambda_j\right|} + O(\|\Delta\boldsymbol{L}\|_2^2),$$

where λ_j (j = 1, 2) represents the other two eigenvalues of the matrix. Thus (eventually) as the points become dense, we can find a constant κ such that if every element of $\Delta\boldsymbol{L}$ is less than ϵ, then $\|\Delta\boldsymbol{v}\|_2 \leq \kappa\epsilon$. This means that—provided the smallest eigenvalue is unique—its eigenvector must also converge from the discrete to continuous case as the points become dense. □

8. CONCLUSIONS

We have presented and proved elegant solutions to the problems of weighted total least-squares fitting of planes and parallel planes. Furthermore, the solutions are conducive to implementation in computer algorithms using reliable and readily available linear algebra functions. The weighted fitting cases can be easily simplified to equally-weighted fitting if desired. The need for such algorithms has been demonstrated

[2] When considering convergence to the continuous case, we treat the surfaces as mathematical, ignoring the fact that, at small scales, the molecular makeup of the material differs from our understanding of the continuous, mathematical surface.

Copyright © 2012 by ASME

and is relevant to newer tolerancing standards and instrumentation.

Furthermore, these fits in the discrete cases converge to their corresponding continuous cases as the points becomes dense (independent of the sampling strategy). This result is not generally true in the case of unweighted fitting.

REFERENCES

[1] International Organization for Standardization (ISO), 2010, "ISO 14405-1:2010, Geometrical product specifications (GPS) - Dimensional tolerancing - Part 1: Linear sizes"

[2] International Organization for Standardization (ISO), "ISO 1101:(future), Geometrical tolerancing – Tolerances of form, orientation, location and run-out"

[3] International Organization for Standardization (ISO), "ISO 14405-3:(future), Geometrical product specifications (GPS) - Dimensional tolerancing - Part 3: Angular sizes"

[4] Parratt, S., and Voelcker, H., 1997, "Do You Know How to Tolerance a Hinge?," mfg., Brown & Sharpe Manufacturing Company, pp. 42-43.

[5] Shakarji, C. M., 1998, "Least-squares fitting algorithms of the NIST algorithm testing system," J. Res. Natl. Inst. Stand. Technol., 103, pp. 633-641.

[6] Forbes, A., "Least-squares best-fit geometric elements," NPL Report, April 1989.

[7] Nievergelt, Y., 1994, "Total least squares: State-of-the-art regression in numerical analysis," SIAM Review, pp. 258-264.

[8] Nievergelt, Y., 2001, "Hyperspheres and hyperplanes fitted seamlessly by algebraic constrained total least-squares," Linear Algebra and its Applications, 331, pp. 43-51.

[9] de Groen, P., 1996, "An Introduction to Total Least Squares," Nieuw Archief voor Wiskunde, Vierde serie, deel 14, pp. 237-253.

[10] Krystek, M., and Anton, M., 2007, "A weighted total least-squares algorithm for fitting a straight line," Meas. Sci. Technol., 18, pp. 3438-3442.

[11] Srinivasan, V., Shakarji, C. M., and Morse, E. P., 2012, "On the Enduring Appeal of Least-Squares Fitting in Computational Coordinate Metrology," ASME Journal of Computing and Information Science in Engineering, 12(1).

[12] Shakarji, C. M., 2011, "Coordinate Measuring System Algorithms and Filters," Coordinate Measuring Machines and Systems, R. J. Hocken, and P. H. Pereira, eds., CRC Press, pp. 153-182.

[13] Krommer, A. R., and Ueberhuber, C. W., 1998, Computational integration, Society for Industrial and Applied Mathematics, Philadelphia.

[14] Stewart, G. W., 1973, Introduction to matrix computations, Academic press, New York.

[15] Meyer, C. D., and Stewart, G. W., 1988, "Derivatives and Perturbations of Eigenvectors," SIAM Journal on Numerical Analysis, 25(3), pp. 679-691.

[16] Watkins, D. S., 1991, Fundamentals of matrix computations, John Wiley and Sons, New York.

Copyright © 2012 by ASME